J. Mol. Biol. (1996) **260**, 224–235

JMB

Nuclear Magnetic Resonance Solution Structure of the Human Hsp40 (HDJ-1) J-domain

Yan Qiu Qian[1]*, Dinshaw Patel[1], F-Ulrich Hartl[2] and Damian J. McColl[2]*

[1]*Cellular Biochemistry and Biophysics Program and* [2]*Howard Hughes Medical Institute, Memorial Sloan-Kettering Cancer Center, 1275 York Avenue NY 10021, USA*

**Corresponding authors*

The J-domain is a highly conserved domain found in all members of the DnaJ family of molecular chaperones. The three-dimensional structure of a recombinant, uniformly ^{15}N-labeled 77-residue polypeptide containing the complete J-domain from human Hsp40 (HDJ-1) has been determined by nuclear magnetic resonance (NMR) spectroscopy in solution. On the basis of 876 upper distance constraints derived from nuclear Overhauser effects (NOE) and 173 dihedral angle constraints, a group of 20 conformers representing the solution structure of the HDJ-1 J-domain was computed with the program DIANA and energy-minimized with the program OPAL. The average of the pairwise root-mean-square deviations of the individual NMR conformers relative to the mean coordinates for the backbone atoms N, C^{α} and C' of residues 4 to 54 and 4 to 66 is 0.88 and 0.99 Å respectively. The molecular architecture includes four helices composed of residues 5 to 9, 15 to 28, 40 to 54 and 60 to 66. A turn composed of residues 10 to 14 links helices I and II, and a loop composed of residues 29 to 39 containing a highly conserved tripeptide HPD (residues 31 to 33) connects the antiparallel helices II and III. The tertiary fold formed by helix I-turn-helix II-loop-helix III forms a closed structural core; the less defined helix IV stands away from the core of the domain. The side-chains of the tripeptide HPD extend out from the core of the structure in the opposite direction from helix IV. The structure supports the hypothesis that the highly conserved tripeptide could play a key role in the interaction of Hsp40 with the molecular chaperone, Hsp70.

Keywords: molecular chaperones; heat shock protein (HSP); protein folding; protein structure; NMR solution structure

Address correspondence to Y. Q. Qian at Department of Physical & Structural Chemistry, SmithKline Beecham Pharmaceuticals, Mail Code UW-2940, PO Box 1539, King of Prussia, PA 19406-0939, USA.

Abbreviations used: Hsp, heat shock protein; HDJ-1, human DnaJ homologue-1; IPTG, isopropyl-β-D-thiogalactopyranoside; NMR, nuclear magnetic resonance; NOE, nuclear Overhauser effect; 2D, two-dimensional; 2QF-COSY, 2D 2-quantum-filtered correlated spectroscopy; TOCSY, 2D total correlation spectroscopy; E.COSY, 2D exclusive correlated spectroscopy; NOESY, 2D nuclear Overhauser effect spectroscopy; HSQC, heteronuclear single quantum coherence; TPPI, time-proportional phase incrementation; REDAC, use of redundant dihedral angle constraints; ppm, parts per million; r.m.s.d., root mean square deviation.

Introduction

Molecular chaperones of the DnaJ (Hsp40) family are found ubiquitously in prokaryotic and eukaryotic cells and play diverse roles in many cellular processes such as translation, translocation and protein folding (reviewed by Cyr *et al*., 1994). In addition to its intrinsic chaperone activity, DnaJ is able to interact directly with and stimulate the ATPase activity of the *Escherichia coli* Hsp70 homologue DnaK (Liberek *et al*., 1991; Langer *et al*., 1992; Szabo *et al*., 1994). DnaJ thus cooperates with DnaK in protein folding and also in mediating assembly and disassembly of macromolecule complexes. Three human DnaJ homologues have been identified, Hsp40 (HDJ-1) (Ohtsuka, 1993), HDJ2 (Chellaiah *et al*., 1993; Oh *et al*., 1993) and

0022–2836/96/270224–12 $18.00/0

HSJ-1 (Cheetham *et al*., 1992) of which HDJ-1 has been the most extensively characterized. Like DnaJ itself, HDJ-1 interacts with Hsp70 and can stimulate its ATPase activity (Freeman *et al*., 1995; Höhfeld *et al*., 1995). HDJ-1 cooperates with the constitutively expressed Hsp70 homologue Hsc70 to mediate efficient refolding of firefly luciferase in an ATP-dependent reaction (Freeman *et al*., 1995). Studies using *in vitro* translation systems have shown that HDJ-1 is associated with a high molecular weight complex that contains translating nascent polypeptide chains, Hsc70 and the Hsp60 homologue TriC (Frydman *et al*., 1994). Immune-depletion of this chaperone from the translation lysate markedly decreases the efficiency of folding of newly translated luciferase. Furthermore, HDJ-1 stimulates the association between Hsc70 and the newly discovered co-chaperone and ATPase regulator, Hip, in a reaction which is dependent on the presence of Mg-ATP (Höhfeld *et al*., 1995). Thus, HDJ-1 plays an important role in protein translation and folding in eukaryotes as well as in the regulation of Hsp70 function.

DnaJ homologues are highly diverse at the primary sequence level but tend to share various combinations of at least three domains (Cyr *et al*., 1994). These three domains appear to correlate with various biochemical functions of the protein (Szabo *et al*., 1995). The most highly conserved domain, the J-domain, is present in all members of the DnaJ family and consists of approximately 70 residues. The other two domains, a glycine/phenylalanine-rich sequence and a cysteine-rich sequence with homology to zinc-finger domains (Szabo *et al*., 1995) are less well conserved. Mutagenesis of a highly-conserved tripeptide (His-Pro-Asp) within the J-domain completely abolishes the ability of *E. coli* DnaJ to stimulate the ATPase activity of DnaK and abrogates its ability to cooperate with DnaK in both refolding and assembly reactions (Wall *et al*., 1994). Thus, it has been proposed that the J-domain plays a critical role in DnaJ-DnaK protein-protein interactions and presumably also in the interaction between HDJ-1 and Hsc70. The backbone fold of the J-domain of *E. coli* DnaJ has been reported (Szyperski *et al*., 1994; Hill *et al*., 1995). We present here the first three-dimensional structure of the J-domain of a eukaryotic DnaJ (Hsp40) family member, HDJ-1. The critical HPD tripeptide is present on a loop of the structure. Intriguingly, in a group of 20 conformers, the side-chains of the histidine and aspartate residues are always oriented away from the structural core of the domain. The implications of this side-chain orientation with respect to interactions with Hsc70 are discussed.

Results and Discussion

Resonance assignments and identification of secondary structure

Nearly complete sequence-specific ^{1}H resonance assignments for the HDJ-1 J-domain (Figure 1) were obtained from the 2D homonuclear spectra using the unlabeled sample following the conventional strategy of a combination of through-bond (2QF-COSY and clean-TOCSY) and through-space (NOESY) connectivities (Billeter *et al*., 1982; Wagner & Wüthrich, 1982; Wider *et al*., 1982; Wüthrich, 1986). However, for Leu10 and Ala11, Ala22 and Tyr23, Ile47 and Ala48, Tyr51 and Asp52, the amide proton resonances of the two neighboring amino acid residues had virtually identical chemical shifts which generated ambiguities in the assignments. Similarly, assignment ambiguities arose for Tyr4 due to the degenerate chemical shifts of its amide proton and δ-proton. The 3D ^{15}N-resolved [^{1}H, ^{1}H] NOESY and the gradient-enhanced 2D [^{15}N, ^{1}H] HSQC spectrum using the subsequently prepared uniformly ^{15}N-labeled domain resolved

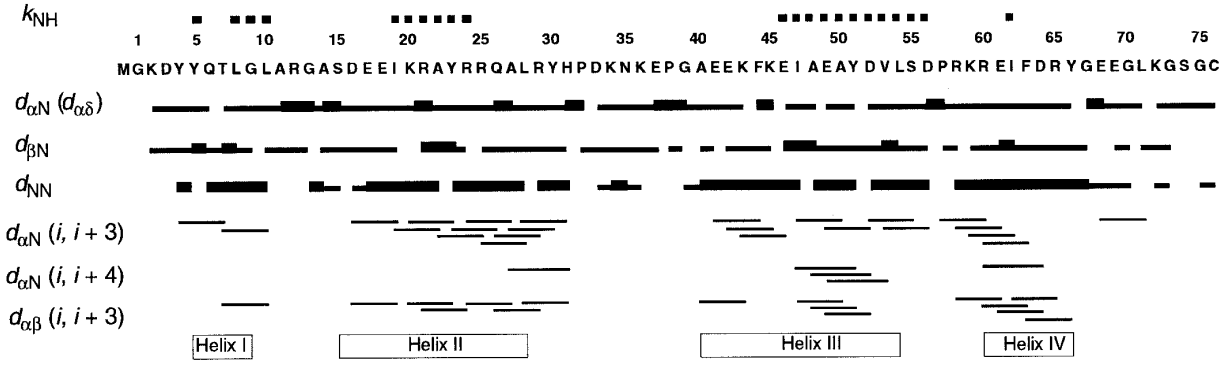

Figure 1. Amino acid sequence of the HDJ-1 J-domain and a survey of the sequential and medium-range NOE connectivities. Filled squares above the sequence identify the locations of amide protons that exchange sufficiently slowly to be observed in a TOCSY spectrum recorded immediately after dissolving the lyophilized protein in $^{2}H_2O$. For the sequential NOE connectivities $d_{\alpha N}$ ($d_{\alpha\delta}$ for Xxx-Pro dipeptide segments), $d_{\beta N}$ and d_{NN}, thick and thin bars indicate strong and weak NOE intensities, respectively; medium-range NOEs are indicated by lines connecting the two residues related by the NOE. The bars at the bottom indicate the locations of secondary structure elements in the HDJ-1 J-domain three-dimensional structure calculated from the NMR data.

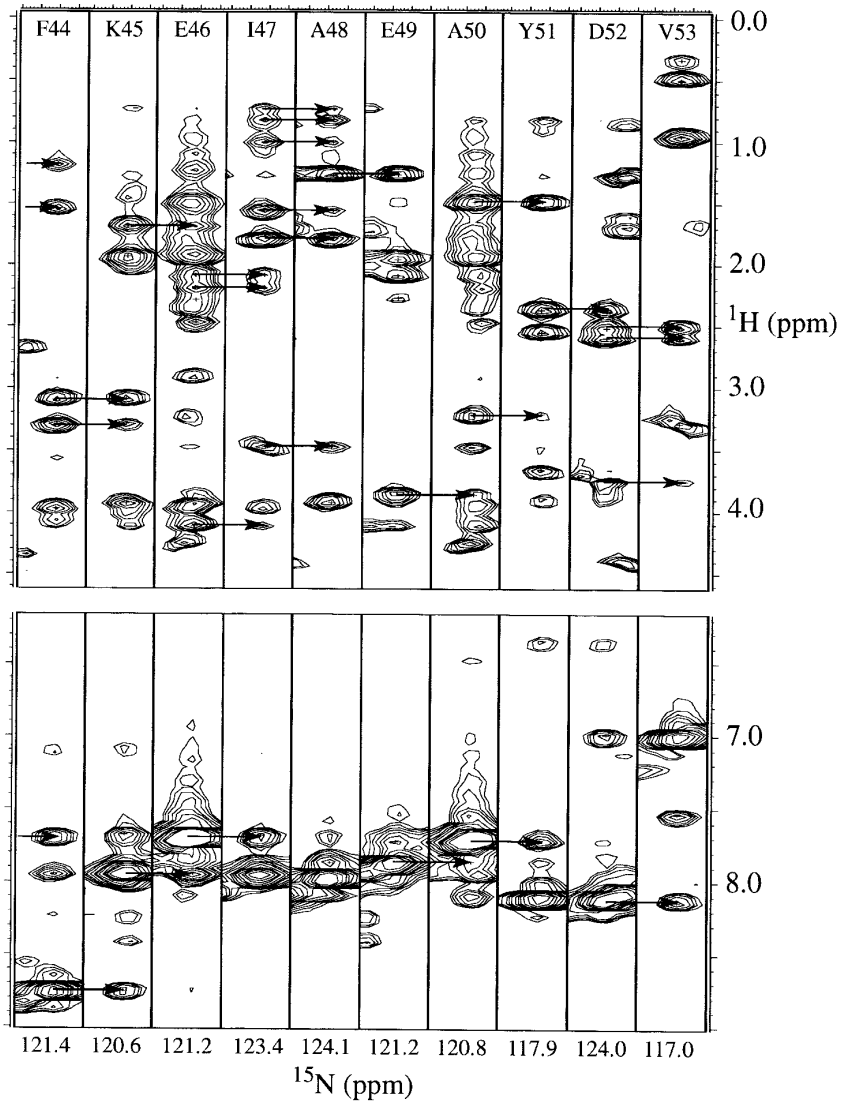

Figure 2. Strip plot taken from the 3D ^{15}N-resolved [^{1}H, ^{1}H] NOESY (uniformly ^{15}N-labeled protein concentration 1.6 mM, solvent 25 mM sodium phosphate, 8 mM perdeuterated dithiothreitol, 90% H_2O/10% ^2H_2O at pH 5.8 and 30°C, mixing time 80 ms, ^{1}H frequency 600 MHz) showing sequential connectivities for residues Phe44 to Val53.

these ambiguities by additional dispersion of the nitrogen-attached protons based on the ^{15}N chemical shifts. The strip plot taken from the 3D ^{15}N-resolved [^{1}H, ^{1}H] NOESY (Figure 2) shows the unambiguous sequential connectivities obtained for residues Phe44 through Val53.

Overall, the proton-bearing backbone ^{15}N chemical shifts were obtained for all residues with the sole exception of the amino-terminal residue Met0. The side-chain ^{15}N chemical shifts were identified for all Asn and Gln residues, and for the ϵ nitrogen atoms of Arg12 and Arg60. For proton resonances, assignments of the non-labile protons in the HDJ-1 J-domain were complete, with the exception of Met0, Pro32, Phe44 and side-chain protons of Arg and Lys residues. Among the labile protons, individual assignments were obtained for all side-chain-NH_2 groups of Asn and Gln residues. Only part of the labile side-chain protons of Arg and Lys residues could be observed. The sequential and intermediate range NOE correlation data observed for backbone NH, αH and βH protons and the secondary structural elements for the HDJ-1 J-domain are summarized in Figure 1.

Two parallel sets of chemical shifts were observed for Asp3, Phe63, Arg65, Tyr66, Glu68, Glu69, and Gly70. In most cases the chemical shift differences between the two sets of lines were within 0.05 ppm with the exception of the amide proton of Glu69 where the difference was 0.43 ppm. A possible explanation for this phenomenon could be the presence of multiple disulfide bonds formed between the C-terminal residue Cys76, which was introduced during the cloning process, and the reducing agent DTT.

Collection of structural constraints and structure calculation

NOE upper distance constraints were collected mainly from two homonuclear NOESY spectra recorded in H_2O or ^2H_2O and supplemented by the heteronuclear 3D ^{15}N-resolved [^{1}H, ^{1}H] NOESY in H_2O to evaluate the overlapped peaks in the

homonuclear spectra. All three spectra were recorded with a mixing time of 80 ms (see Materials and Methods for details). The NOE cross-peak volumes determined with the program XEASY (Bartels *et al*., 1995) were calibrated to establish the corresponding proton-proton distance constraints (Güntert *et al*., 1991b). The program ASNO was used to check constraints with consistent violations in the preliminary structures for possibly incorrect NOESY cross-peak assignments or integrations (Güntert *et al*., 1993). In total, 1187 NOEs were assigned in the three NOESY spectra. In addition, 65 $^3J_{HN\alpha}$ coupling constants were measured by inverse Fourier transformation of the in-phase multiplets in the gradient enhanced 2D [^{15}N, ^{1}H] HSQC spectrum (Szyperski *et al*., 1992), and 38 $^3J_{\alpha\beta}$ coupling constants representing unique rotamer states (Nagayama & Wüthrich, 1981) were measured from an E. COSY spectrum recorded in ^2H_2O. After the initial processing with HABAS (Güntert *et al*., 1989) and DIANA (Güntert *et al*., 1991a), the input data for the DIANA structure calculations consisted of 876 relevant NOE upper distance limits on proton-proton distances and 173 constraints on the dihedral angles ϕ, ψ and χ^1. Stereospecific assignments for 32 non-degenerate βCH_2, γCH_2 and δCH_2 proton pairs, and two pairs of isopropyl methyl groups (Table 1) were obtained with the programs HABAS and GLOMSA (Güntert *et al*., 1991a,b). For all three NH_2 groups of Gln and Asn residues individual assignments were determined from the relative intensity of the NOEs to the nearest CH_2 group in the covalent structure. The sequence and range distributions of the NOE distance constraints are shown in Figure 3. The substantial number of medium-range and long-range NOE distance constraints indicated that the structure of the HDJ-1 J-domain would be well determined by NMR data. The lack of NOE distance constraints for the N-terminal and the C-terminal segments (Figure 3) indicated that the conformation of the two chain termini would not be well determined after the structure calculation.

The final DIANA calculations were started with 50 randomized conformers. One REDAC cycle (Güntert & Wüthrich, 1991) was applied, followed by a computation at the maximum target level using only the original 173 dihedral angle constraints obtained with HABAS. Among the 50 computed conformers, the best 20 solutions had values of the DIANA target function in the range 0.94 to 2.11 Å^2 (Table 1). For each of these 20 DIANA conformers, restrained energy-minimization with the program OPAL yielded a low-energy conformation with further reduced maximum constraint violations and only a small increase in the sum of constraint violations (Table 1). The pairwise r.m.s.d. values of the 20 conformers relative to their mean before and after energy minimization were virtually unchanged, independent of the atoms selected for the r.m.s.d. calculation (Table 1).

Table 1. Analysis of the 20 DIANA conformers representing the solution structure of the HDJ-1 J-domain before and after energy minimization with the program OPAL

Parameter	DIANA[a,c]	DIANA + OPAL[b,c]
DIANA target function (Å^2)	1.53 ± 0.34 (0.94–2.11)	
NOE violations		
Number >0.1 Å	18.0 ± 4.0 (12–27)	0.4 ± 0.6 (0.0–2.0)
Sum of violations (Å)	5.9 ± 0.8 (4.8–7.4)	6.7 ± 0.4 (6.1–7.4)
Maximum violation (Å)	0.34 ± 0.14 (0.17–0.60)	0.10 ± 0.01 (0.09–0.11)
Dihedral angle constraint violations		
Number >2.5°	3.5 ± 0.9° (1.0–5.0)	0.2 ± 0.4° (0.0–1.0)
Sum of violations (deg.)	28.0 ± 4.2° (21.3–35.8)	32.9 ± 4.2° (25.5–41.5)
Maximum violation (deg.)	5.3 ± 1.6° (3.1–7.9)	2.2 ± 0.3° (1.9–2.8)
AMBER energy (kcal/mol)		
Physical energies	–2046 ± 124 (–2261– –1851)	–3442 ± 81 (–3584– –3221)
Van der Waals energy	609 ± 79 (465–772)	– 217 ± 15 (–238– –187)
Electrostatic energy	–3303 ± 78 (–3455– –3174)	–3791 ± 80 (–3934– –3584)
R.m.s.d. values (Å)		
Backbone N, C$^\alpha$, C' (5–9, 15–28, 40–54)[d]	0.56 ± 0.11 (0.37–0.74)	0.56 ± 0.12 (0.40–0.81)
Same + 15 best side-chains[d,e]	0.65 ± 0.12 (0.45–0.90)	0.60 ± 0.14 (0.43–0.98)
Same + all heavy atoms[d]	1.20 ± 0.11 (1.05–1.44)	1.21 ± 0.11 (1.07–1.44)
Backbone N, C$^\alpha$, C' (4–54)[d]	0.89 ± 0.22 (0.62–1.34)	0.88 ± 0.21 (0.62–1.36)
Same + 15 best side-chains[d,e]	0.92 ± 0.19 (0.65–1.28)	0.88 ± 0.19 (0.61–1.29)
All heavy atoms (4–54)[d]	1.46 ± 0.20 (1.20–1.86)	1.45 ± 0.20 (1.15–1.83)
Backbone N, C$^\alpha$, C' (4–66)[d]	1.02 ± 0.24 (0.62–1.46)	1.01 ± 0.22 (0.66–1.39)
Same + 15 best side-chains[d,e]	1.02 ± 0.21 (0.64–1.40)	0.99 ± 0.20 (0.64–1.33)
All heavy atoms (4–66)[d]	1.60 ± 0.22 (1.19–1.97)	1.57 ± 0.20 (1.21–1.92)

[a] DIANA conformers before energy minimization.
[b] DIANA conformers after energy minimization with the program OPAL.
[c] The numbers given are the mean values ± standard deviations, with the minimum and maximum values among the 20 conformers given in parentheses. The r.m.s.d. values are relative to the mean of the 20 best conformers.
[d] The numbers in parentheses indicate the amino acid residues used to calculate the r.m.s.d.
[e] Includes the backbone atoms N, C$^\alpha$ and C' of the residues indicated, and the side-chain heavy atoms of the 15 best-defined residues, 4, 7, 10, 14 to 15, 19, 22, 27, 44, 47 to 48, 50 to 51, 53 to 54 (see the text).

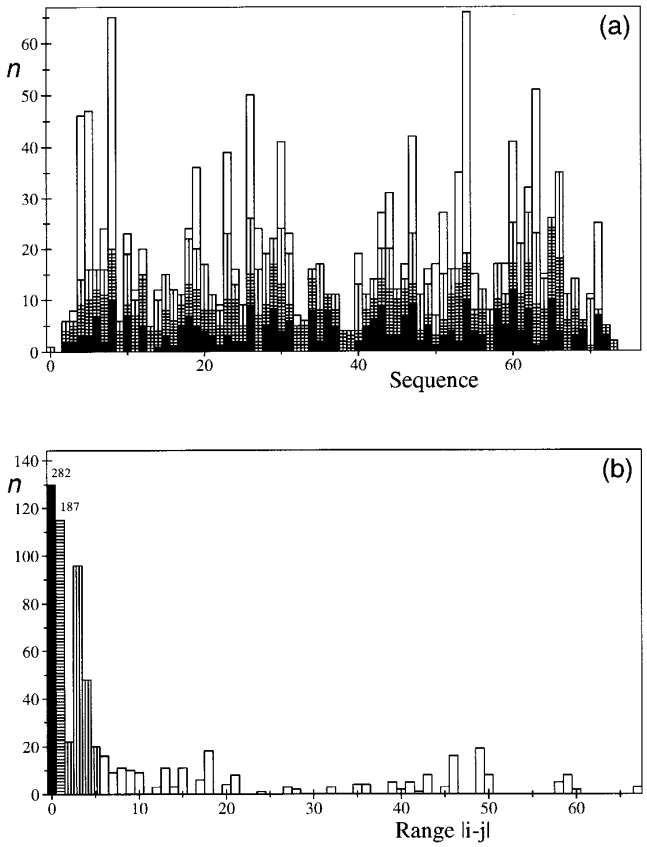

Figure 3. Range and sequence distribution of the NOE constraints used in the calculation of the HDJ-1 J-domain structure. (a) Number of NOE distance constraints per residue, *n*, *versus* the amino acid sequence. The constraints are specified as follows: black, intra-residual; crosshatched, constraints between protons in sequentially neighboring residues; vertically hatched, medium-range constraints between protons located in residues separated by two to five positions along the sequence; white, all longer-range constraints. (b) Number of NOE constrains, *n*, as a function of the separation along the amino acid sequence of the residues containing the hydrogen atoms between which the NOE is observed. Black, intra-residual; crosshatched, sequential NOEs (since these plots would go off-scale, the number of intra-residual and sequential NOEs are indicated at the top of the Figure); vertically hatched, medium-range NOEs (two to five residues separation); white, long-range NOEs (>five residues separation).

The NMR solution structure of the HDJ-1 J-domain

Figure 4 shows a superposition for the polypeptide backbone of the 20 DIANA conformers of the HDJ-1 J-domain after restrained energy minimization. The two terminal residues were unstructured as expected due to the lack of NMR data. The defined part of the domain contains residues 4 to 66 which comprise four helices composed of residues 5 to 9, 15 to 28, 40 to 54 and 60 to 66. Helix I from residues 5 to 9 is a 3_{10}-helix since O'-HN hydrogen bonds between residues 5 to 8 and 6 to 9 were observed. The other three are α-helical helices. A pentapeptide (residues 10 to 14) forms a turn linking helix I to helix II. The axis of helix I forms an angle of about 45° with respect to the axis of helix II and crosses the axis of helix II at a point between the second and third turn. Helix II is connected by a loop composed of residues 29 to 39 leading to helix III, and the two helices are oriented in an anti-parallel fashion with respect to one another. The tertiary fold helix I-turn-helix II-loop-helix III forms the structural core of the HDJ-1 J-domain. The less well-defined helix IV is connected to helix III by a turn composed of residues 55 to 59 and is oriented approximately orthogonal to helix III, facing away from the core of the domain (Figure 4).

A characterization of the local features of the NMR structure of the HDJ-1 J-domain is presented in Figure 5 which shows the global displacements between the mean atom coordinates and the individual conformers. The backbone atoms of helices I, II and III are defined precisely whereas the turn linking helix I to helix II and the loop connecting helix II and helix III are less well-characterized. The fourth helix is apparently more disordered. A further assessment of the precision of different segments is provided by the global r.m.s.d. values (Table 1). The value of the average r.m.s.d. calculated for the backbone atoms N, C^{α} and C' of helix I (residues 5 to 9), helix II (residues 15 to 28) and helix III (residues 40 to 54) is 0.56($\pm$0.12) Å representative of a high-quality NMR structure determination. A nearly identical value is obtained when the 15 best-defined side-chains (listed in Table 1; for these residues the global side-chain displacement, D^{sc}_{glob}, is less than 1.47 Å) are also considered. The r.m.s.d value of 0.88 Å for the backbone atoms of residues 4 to 54 indicates that the turn (linking helix to helix 2) and the loop (connecting helix II to helix III) are less-defined. Addition of residues 55 to 66 results in an increased r.m.s.d. value of 1.01 Å for the backbone atoms of residues 4 to 66, highlighting the thermally dynamic state of helix IV.

A direct visualization of the molecular core of the HDJ-1 J-domain is presented in Figure 6, representing a superposition of 20 conformers containing the entire backbone from residues 4 to 54 and including the 15 well-defined side-chains located in the interior of the domain. As is generally observed in globular proteins in solution, the surface side-chains (Figure 5(b)) are distinctly less well-defined by the NMR data, which is also manifested in a significant increase of the global r.m.s.d. value calculated for all heavy atoms (Table 1).

Functional implications of the HDJ-1 J-domain structure

The structural features of the HDJ-1 J-domain are very similar to that of the previously reported backbone fold of the homologous domain from *E. coli* DnaJ (Szyperski *et al*., 1994; Hill *et al*., 1995) with slight differences in the helix termini. The

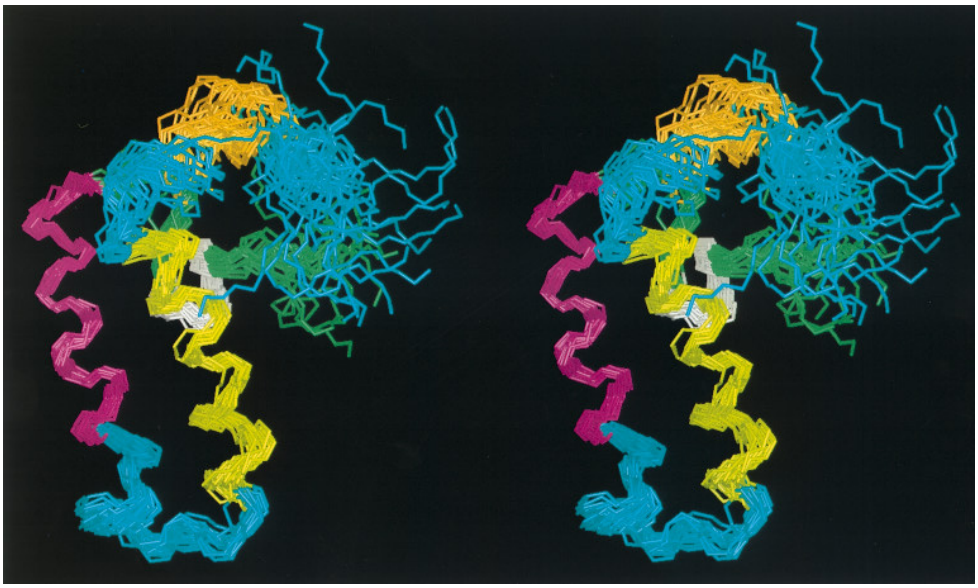

Figure 4. Stereo view of the polypeptide backbone atoms N, C^{α} and C' for the 20 energy-refined DIANA conformers of the HDJ-1 J-domain. The superposition was taken for best fit of the backbone atoms N, C^{α} and C' of residues 4 to 54. The color coding is: residues 0 to 3, 10 to 14, green; 4 to 9 (helix I), white; 15 to 28 (helix II), magenta; 40 to 54 (helix III), yellow; 60 to 66 (helix IV), orange; 29 to 39, 55 to 59 and 67 to 76, cyan.

orientation of helix IV relative to the core of the HDJ-1 J-domain formed by helix I to helix III more closely resembles that of Hill *et al*. (residues 1 to 78) than that of Szyperski *et al*. (residues 2 to 108). The substantial number of long-range NOEs from helix IV (Figure 3(a)) to helices I, II and III resulted in the unique orientation of helix IV relative to the core of the domain as shown by the ribbon drawing (Figure 7). Among these inter-helical NOEs, Arg60 makes five NOEs to Ile19 (helix II), three NOEs to Val53 (III) and eight NOEs to Leu54 (III); Phe63 makes two NOEs to Asp3 (I), seven NOEs to Tyr4 (I), five NOEs to Tyr5 (I), three NOEs to Val53 (III) and three NOEs to Leu54 (III) and Asp64 makes one NOE to Tyr5 (I).

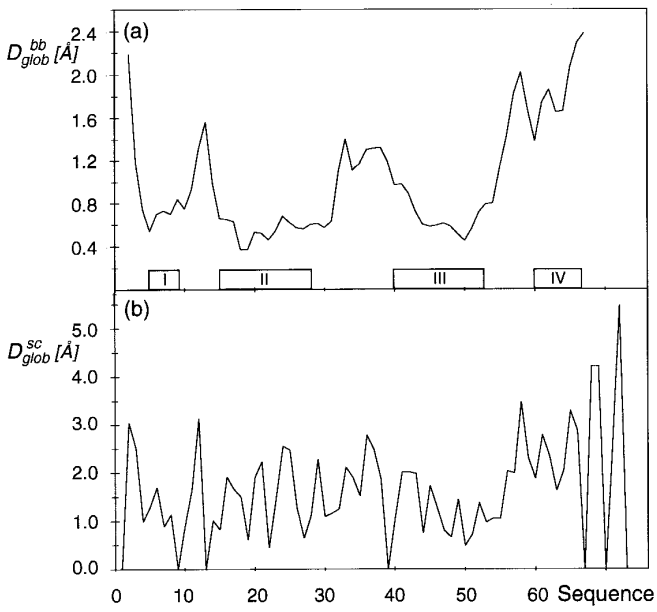

Figure 5. Plots of global displacement, D_{glob}, *versus* the amino acid sequence (Billeter *et al*., 1989) for individual amino acid residues between the 20 energy-refined DIANA conformers of the HDJ-1 J-domain and the mean coordinates. Before calculating the displacements, the backbone atoms N, C^{α} and C' of residues 4 to 54 were superimposed for optimal fit. (a) D^{bb}_{glob} calculated for the backbone atoms N, C^{α} and C'. (b) D^{sc}_{glob} calculated for all side-chain heavy atoms.

The J-domains of *E. coli* DnaJ and HDJ-1 share approximately 50% sequence identity. A sequence alignment of 14 J-domains from numerous species is shown in Figure 8. It is of interest to note that many highly conserved residues are associated with the structural core of the J-domain. These include Ala14, Ile19, Ala27, Phe44, Ala50, Tyr51 and Leu54, which were well-defined in the structure of the HDJ-1 J-domain (Table 1, Figure 6). Thr7, Ala22, Ile47 and Val53 are also involved in stabilizing the structural core of the HDJ-1 J-domain and although not absolutely conserved, appear to tolerate only conservative substitutions. Several charged residues are highly conserved or tolerate only conservative substitutions (positions 20, 21, 24, 43, 46, 56, 59 and 64) and are likely candidates for interactions with Hsp70. Other less well conserved residue positions (corresponding to Glu17 in helix II and Lys45 in helix III) have been implicated in playing a role in determining the specificity of the interaction of Hsp70 with DnaJ/HDJ-1 homologues (Schlenstedt *et al*., 1995). The HDJ-1 J-domain structure also provides some insight into the nature of a mutant of the yeast DnaJ homologue Sec63 which fails to interact with Kar2p, the endoplasmic reticulum Hsp70 homologue (Lyman & Schekman, 1995). This mutant, A181T, corresponds to the highly conserved Ala50

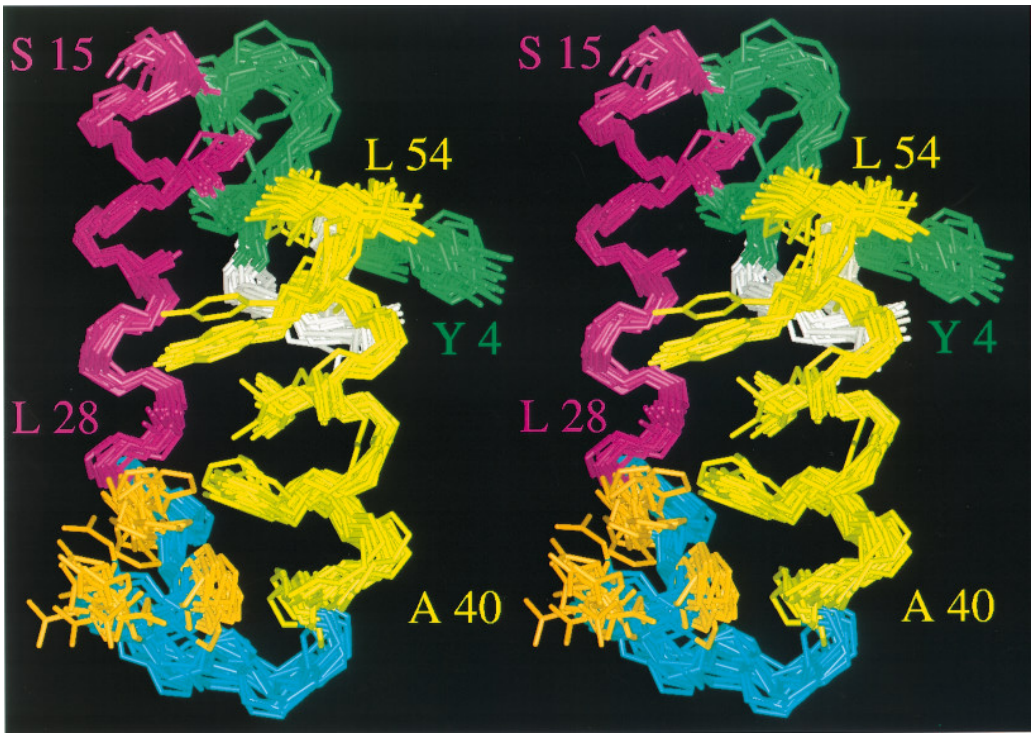

Figure 6. Stereo views of the superposition of the backbone atoms N, C^{α} and C' of residues 4 to 54 for the 20 energy-refined DIANA conformers characterizing the structural core of the HDJ-1 J-domain. The polypeptide backbone and heavy atoms of the 15 best-defined side-chains (residues 4, 7, 10, 14, 15, 19, 22, 27, 44, 47, 48, 50, 51, 53 and 54) and of the highly conserved tripeptide His31-Pro32-Asp33 are shown. The color codes are as in Figure 6 with the exception of the side-chains of the tripeptide which are shown in orange. Some sequence positions are identified with numbers.

in HDJ-1 which is located within the hydrophobic core of the domain and makes extensive long-range NOEs with Tyr4 and Thr7 on helix I. Substitution of this residue probably destabilizes both interactions between the N-terminal end of helix I and the C-terminal end of helix III as well as disrupting the antiparallel packing of helix II and helix III.

The most striking feature of the HDJ-1 J-domain structure is the location of the absolutely conserved tripeptide His31-Pro32-Asp33 on the surface of the loop connecting helix II and helix III. The r.m.s.d. value for the backbone atoms of this loop, composed of residues 29 to 39, is 0.72 Å, and it increases only slightly to 0.88 Å when the heavy atoms of the three side-chains of His31-Pro32-Asp33 are included. This indicates that the loop is well-defined locally. It is interesting to see that the side-chains of the conserved tripeptide His31-Pro32-Asp33 are facing away from the core of the J-domain (Figures 6, 7). The orientation of these residues is due to observed NOEs between their side-chain protons and the protons of neighboring residues (e.g. His31 H^{β}-Leu28 H^{α}, His31 H^{δ}-Leu28 H^{α}, Pro32 H^{γ}-His31 H^{α} and Asp33 H^{β}-His31 H^{ϵ}). Thus we propose that this tripeptide may be involved in mediating the interaction between HDJ-1 and Hsp70. Although HDJ-1 has not been the subject of mutational analysis, the position and orientation of the HPD tripeptide in the J-domain of HDJ-1 would explain several mutants which have been described in DnaJ and in the DnaJ homologue Sec63. One such mutant, DnaJ259, is a point mutant that contains a H33Q substitution (corresponding to His31 of HDJ-1; Wall *et al*., 1994). This mutant cannot stimulate the ATPase activity of DnaK, the Hsp70 homologue of *E. coli*, nor can it alter the conformation of DnaK in the presence of ATP. In Sec63, P157N and D158A substitutions (corresponding to Pro32 and Asp33 in HDJ-1) result in a translocation stalling defect (Feldheim *et al*., 1992). These mutations probably inhibit the interaction of Kar2p with Sec63, which is necessary for the completion of polypeptide translocation into the endoplasmic reticulum.

The sequences following the HPD tripeptide and forming the remainder of the loop are highly variable among the HDJ-1 homologues (Figure 8) with the exception of residues 34 and 35 which are well conserved. Whether such variation plays a role in determining the specificity of Hsp40 / Hsp70 interactions or simply represents mutations in a functionally neutral sequence remains to be clarified. The conserved proximity of the HPD tripeptide to the C-terminal end of helix II and the highly charged nature of this helix suggests the possibility that these two regions form a charged binding interface between HDJ-1 and Hsp70. Intriguingly, the mitochondrial protein MIM44, which interacts with mitochondrial Hsp70 in translocating polypeptide chains through the mitochondrial membranes, has a very short region of homology to the J-domain corresponding only to

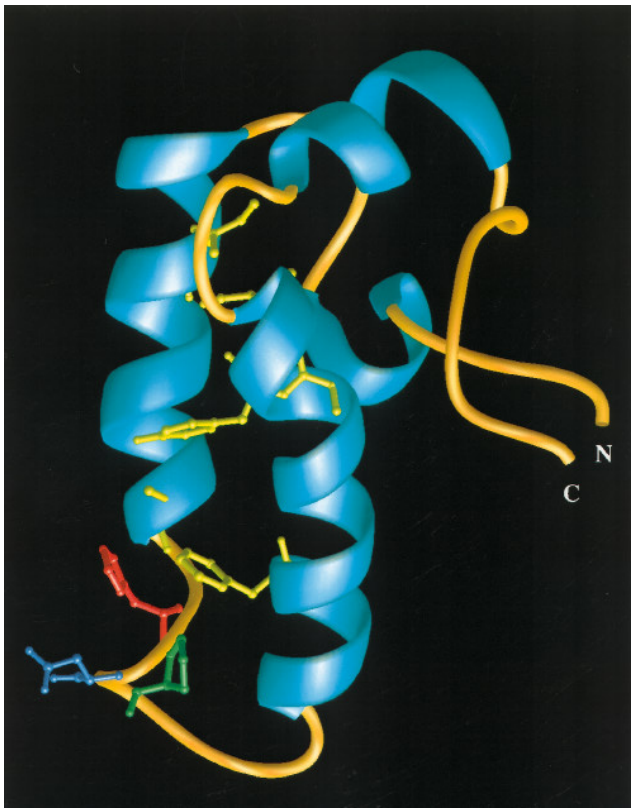

Figure 7. Ribbon drawing of one energy refined DIANA conformer of the HDJ-1 J-domain (residues 0 to 76). The chain termini are identified by the letters N and C. Helices I to IV are shown in cyan, the loop and turns connecting the helices are shown in orange. The HPD tripeptide is indicated by the residues in red (His31), green (Pro32) and blue (Asp33). Six highly conserved residues (positions 19, 27, 44, 50, 51 and 54) involved in the stabilization of the structural core of the J-domain are indicated in yellow.

helix II and the HPD motif (although the sequence in MIM44 is NED; Rassow *et al*., 1994). This suggests that the combination of helix II and the HPD tripeptide may be the minimal sequence required for binding to Hsp70 proteins. Other regions of the J-domain may also be involved in interactions with Hsp70. Helix IV is less ordered compared to the other three helices in the J-domain. Asp64 in helix IV is highly conserved and may play a role in the J-domain / Hsp70 interaction. We noted that in 9 out of 20 conformers, a potential 3_{10}-helix may exist from residues 67 to 71 as O' -HN hydrogen bonds were observed between residues 67 to 70 and 68 to 71. Whether this potential 3_{10}-helix becomes an extension of helix IV in the HDJ-1 / Hsp70 complex or simply represents a transient conformer remains to be clarified.

Other interactions between chaperones may also be mediated by exposed loop structures. In the *E. coli* system, a small surface-exposed loop on the ATPase domain of DnaK has been proposed to be critical for the interaction of DnaK with its nucleotide exchange factor, GrpE (Buchberger *et al*., 1994). The sequence of this loop structure is relatively well conserved in eukaryotic homologues of DnaK but no direct homologue of GrpE has been identified in eukaryotes. Hip, an ATPase regulator and co-chaperone of mammalian Hsc70 does bind to the ATPase domain of Hsc70 (Höhfeld *et al*., 1995), but the role of the conserved loop, if any, in this interaction remains to be established.

J-domains have also been identified in several proteins other than molecular chaperones. These include auxilin, a cofactor in the Hsc70-dependent uncoating reaction of clathrin-coated vesicles (Ungewickell *et al*., 1995); the SV40 and polyoma virus T antigens which bind Hsp70 and are involved in viral replication (Kelly & Landry, 1994), and cysteine string proteins which function in synaptic vesicle transmission (Zinsmaier *et al*., 1994). Thus the J-domain may be a generalized module for concentrating Hsp70 at sites where its ability to bind and release polypeptide is utilized in a variety of cellular processes.

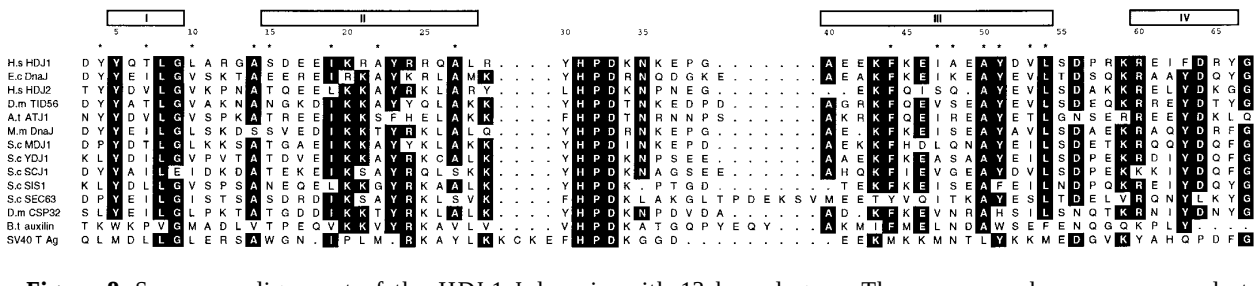

Figure 8. Sequence alignment of the HDJ-1 J-domain with 13 homologues. The sequence shown corresponds to residues 3 to 67 of the HDJ-1 J-domain. Residues conserved in at least 10 of the 14 J-domains are outlined in black. Numbers above the sequence correspond to the residue position in the HDJ-1 J-domain. Rectangles above the sequences correspond to the four helices in the HDJ-1 J-domain and are numbered accordingly. Asterisks indicate the residues in the HDJ-1 J-domain for which the side-chains were well defined in the structure (see foot note of Table 1). Abbreviations are H.s, *Homo sapiens*; E.c, *Escherichia coli*; D.m, *Drosophila melanogaster*; A.t, *Aradopsis thaliana*; M.m, *Methanosarcina mazeii*; S.c, *Schizosacchromyces cerevisiae*; B.t, *Bos taurus*. Accession numbers for the listed proteins are: D17749 (H.s HDJ1), P08622 (E.c DnaJ), L08069 (H.s HDJ2), X77822 (D.m TID56), U16246 (A.t ATJ1), S75267 (M.m DnaJ), Z28336 (S.c MDJ1), X56560 (S.c YDJ1), X58679 (S.c SCJ1), X58460 (S.c SIS1), X16388 (S.c SEC63), M63421 (D.m CSP32), U09237 (B.t auxilin), P03081 (SV40).

Materials and Methods

Cloning and over-expression of the HDJ-1 J-domain

The nucleotide sequence of the HDJ-1 J-domain (residues 1 to 76) was amplified by polymerase chain reaction (PCR; Saiki *et al*., 1988) using 1 ng of a full length HDJ-1 clone in the vector pQE9 as template DNA (Y. Minami, K. Ohtsuka, and F. U. Hartl, unpublished). The oligonucleotide primers 403 (5'-GAGTCACATAT-GGGTAAAGACTACTAC-3') and 404 (5'-GATTATG-GATCCCTTTAGGCCTTCCTC-3') were used to prime the template DNA. The resulting 243 bp PCR product was purified on 1.5% (w/v) low melting point (LMP) agarose (NuSieve GTG, FMC), digested with the restriction endonucleases *Nde*I and *Bam*HI (Boehringer), and ligated into the expression vector pET3a (Novagen). HDJ-1 J-domain clones in pET3a were transformed into *E. coli* TG1 cells and grown on 2×YT agar containing 50 μg/ml ampicillin. Plasmid DNA was prepared from several of the resulting transformants using TIP-20 columns (Qiagen). Nucleotide sequencing of the resulting clones was performed using standard protocols (USB Chemicals) and confirmed that the amplified sequence corresponded to the published HDJ-1 nucleotide sequence (Ohtsuka, 1993). A cysteine codon was introduced at the 3' end of the HDJ-1 J-domain as a result of the cloning process. One of the resulting clones, 40J-6 was transformed into *E. coli* BL21 DE3 pLysE cells (Novagen). Individual transformants were grown overnight at 37°C in 2×YT medium containing 150 μg/ml ampicillin and 50 μg/ml chloramphenicol, then diluted 1:100 and grown to an optical density at 600 nm of 0.2. Expression of the HDJ-1 J-domain was induced by addition of IPTG to the cultures at a final concentration of 1 mM followed by a further incubation at 37°C for four hours.

Purification of unlabeled and uniformly ^{15}N-labeled HDJ-1 J-domain

Cells expressing the HDJ-1 J-domain were subjected to centrifugation at 6000 ***g*** (Sorvall GS3 rotor). Cell pellets were resuspended in buffer A (50 mM Tris-HCl (pH 8.0), 10% sucrose, 10 mM DTT, 10 mM EDTA, 1 mM PMSF, 1 mg/ml lysozyme, 7.5 μg/ml DNase I) at a final suspension of 1 g cells/ml buffer A. Cells were lysed by incubation at 4°C for one hour with mixing followed by sonication. The lysate was subjected to ultracentrifugation at 70,000 ***g*** at 4°C for one hour (Beckmann Ti45 rotor), the supernatant harvested, and subjected to ammonium sulfate precipitation at 60% saturation. The precipitate was subjected to ultracentrifugation as above and the supernatant containing the soluble HDJ-1 J-domain collected and dialyzed against buffer B (50 mM Na_2HPO_4, pH 10.0, 10 mM DTT) at 4°C for 24 hours. The dialyzed supernatant was loaded onto a Q-Sepharose (Pharmacia) anion exchange column. The column was washed with five column volumes of buffer B and the flow-through fractions containing the HDJ-1 J-domain were collected. These fractions were pooled and subjected to reverse-phase HPLC (Rainin HPXL) on a C4 column (Vydac, 1.0 cm × 25 cm) with an initial gradient of 2% acetonitrile/0.1% TFA/min from 5% to 95% acetonitrile. Fractions containing the HDJ-1 J-domain were collected, lyophilized, resuspended in buffer B and subjected to a second purification step by RP-HPLC using a gradient of 1% acetonitrile/0.1% TFA/min from 0% to 60% acetonitrile. The resulting HDJ-1 J-domain was lyophilized and resuspended in buffer B. The protein concentration was estimated by measurement of the absorbance at 280 nm (extinction coefficient, 8914 M^{-1} cm^{-1}). The HDJ-1 J-domain was concentrated to at least 1 mM in a volume of 0.6 ml by buffer exchange over a YM3 membrane (Amicon).

Uniformly ^{15}N-labeled HDJ-1 J-domain was prepared by growth of BL21 DE3 pLysE 40J-6 cells overnight in 2×YT as described above, followed by transfer into minimal labeling medium for induction. One liter labeling medium contained KH_2PO_4, 13 g; K_2HPO_4, 10 g; Na_2HPO_4, 9 g; K_2SO_4, 2.4 g; $^{14}NH_4Cl$ or $^{15}NH_4Cl$, 1 g; ampicillin 150 μg/ml, chloramphenicol, 50 μg/ml, 0.5% (w/v) glucose, 5 mM $MgCl_2$, 0.001% (w/v) thiamine-HCl and 5 ml trace element solution (100 ml stock solution: $CaCl_2{\cdot}2H_2O$, 0.6 g; $FeSO_4{\cdot}7H_2O$, 0.6 g; $MnCl_2{\cdot}4H_2O$, 0.12 g, $CoC1_2{\cdot}6H_2O$, 80 mg; $ZnSO_4{\cdot}7H_2O$, 70 mg; $CuCl_2{\cdot}2H_2O$, 30 mg, H_3BO_3, 2 mg; $(NH_4)_6Mo_7O_{24}{\cdot}4H_2O$, 25 mg; EDTA, 0.5 g). Cells were first ''starved'' for 1.5 hours in medium containing $^{14}NH_4Cl$, harvested by centrifugation as above and transferred to $^{15}NH_4Cl$-containing labeling medium. Following addition of IPTG each one liter culture was supplemented with 25 ml of 20% glucose at 1.5 hour intervals over a six hour time course of induction. Cells were harvested as above and purification of the ^{15}N-labeled HDJ-1 J-domain was performed as above.

NMR measurements

NMR measurements were performed on Varian Unity Plus 600 spectrometers equipped with a self-shielded z-gradient probe. Two NMR samples, a uniformly ^{15}N-labeled and an unlabeled HDJ-1 J-domain, were prepared in the same solution conditions: ~1.6 mM protein, 25 mM sodium phosphate, 8 mM perdeuterated dithiothreitol, 90% H_2O/10% ^2H_2O at pH 5.8 and 30°C. The following 2D homonuclear experiments were recorded in both H_2O and ^2H_2O solution: 2QF-CO-SY, clean-TOCSY (Griesinger *et al*., 1988) with a mixing time of 80 ms, and NOESY (Anil-Kumar *et al*., 1980) with a mixing time of 80 ms. In addition, an E. COSY spectrum (Griesinger *et al*., 1985) was recorded in ^2H_2O. Typical data sizes were 400×1024 complex points in t_1 and t_2, respectively. Two heteronuclear spectra were recorded with the uniformly ^{15}N-labeled sample: a 3D ^{15}N-resolved [^{1}H, ^{1}H] NOESY (Fesik & Zuiderweg, 1988) with a mixing time of 80 ms, data size of 170×40×512 complex points and a total recording time of 85 hours, and a gradient-enhanced 2D [^{15}N, ^{1}H] HSQC spectrum (Kay *et al*., 1992) with a data size of 128×2048 complex data points. For both the homonuclear and heteronuclear experiments, the States-TPPI method (Marion *et al*., 1989) was used for obtaining the phase-sensitive mode in the indirectly detected dimension. For the experiments in H_2O, the water signal was suppressed by selective saturation (Wider *et al*., 1983). Data were processed with the VNMR software, version 5.1 (Varian Associates). Before Fourier transformation, the time domain data were multiplied with a shifted Gaussian bell filter in the directly detected dimension and with a shifted sine bell filter in the indirectly detected dimensions. Baseline distortions were corrected using the program FLATT (Güntert & Wüthrich, 1992).

Slowly exchanging amide protons were identified in a homonuclear TOCSY spectrum recorded with a mixing time of 80 ms, where the lyophilized protein was dissolved in ^2H_2O immediately before starting the NMR measurement. The program XEASY (Bartels *et al*., 1995)

was used for peak picking, and for the integration of the cross peaks in the homonuclear and heteronuclear NOESY spectra. Vicinal scalar coupling constants $^3J_{HN\alpha}$ were extracted by inverse Fourier transformation of in-phase multiplets (Szyperski *et al*., 1992) from the gradient-enhanced 2D [^{15}N, ^{1}H] HSQC spectrum. $^3J_{\alpha\beta}$ scalar coupling constants were measured in the E. COSY spectrum that was zero-filled to 4096 data points in t_2 prior to Fourier transformation.

Determination of the three-dimensional structure

The structure calculations were performed with the program DIANA (Güntert *et al*., 1991a). One REDAC cycle (Güntert & Wüthrich, 1991) was used for improved convergence. Upper distance constraints were obtained from cross-peak volumes measured in the aforementioned three NOESY spectra (2D homonuclear NOESY spectra in H_2O and ^2H_2O, and the 3D ^{15}N-resolved [^{1}H, ^{1}H] NOESY) using the program CALIBA (Güntert *et al*., 1991a). No hydrogen bond constraints were used during the structure calculations. Dihedral angle constraints and stereospecific assignments for β-methylene groups were determined from the spin-spin coupling constraints and assignments for β-methylene groups were determined from the spin-spin coupling constraints and the intraresidual and sequential NOEs using the program HABAS (Güntert *et al*., 1989). Further stereospecific assignments of βCH_2 and of other pairs of diastereotopic substituents were obtained with the program GLOMSA (Güntert *et al*., 1991a,b). Restrained energy-minimization was performed in a water shell for 1500 conjugate gradient steps using the program OPAL (P. Luginbühl, P. Güntert, M. Billeter & K. Wüthrich, unpublished), which employs the AMBER 94 force field (Weiner *et al*., 1986) and further includes pseudo-energy terms for distance constraints and dihedral angle constraints (Billeter *et al*., 1989). The pseudo-energy was proportional to the the power of the distance constraint violations, and it was adjusted such that violations of 0.1 Å for distance constraints and 2.5° for dihedral angle constraints corresponded to $k_BT/2$ at room temperature. There was no cutoff used for non-bonded interactions during restrained energy minimization. The structural analysis was performed with the program XAM (Xia 1992).

Acknowledgements

We thank Drs P. Güntert for valuable advice on the structure calculation; T.-H. Xia for advice on the data processing; S. Geromonas, J. Hendrick and J. Frydman for advice and assistance with purification of the HDJ-1 J-domain and R. Ajay Kumar and John Hubbard for help producing the color Figures. Financial support was obtained from start up funds to D.J.P. from the Memorial Sloan-Kettering Cancer Center. D.J.M. was supported by the Howard Hughes Medical Institute.

References

Anil Kumar, Ernst, R. R. & Wüthrich, K. (1980). A two-dimensional nuclear Overhauser enhancement (2D NOE) experiment for elucidation of complete proton-proton cross-relaxation networks in biological macromolecules. *Biochem. Biophys. Res. Commun.* **95**, 1–6.

Bartels, C., Xia, T.-H., Billeter, M., Güntert, P. & Wüthrich, K. (1995). The program XEASY for computer-supported NMR spectral analysis of biological macromolecules. *J. Biomol. NMR*, **6**, 1–10.

Billeter, M., Braun, W. & Wüthrich, K. (1982). Sequential resonance assignments in protein ^{1}H nuclear magnetic resonance spectra. Computation of sterically allowed proton-proton distances and statistical analysis of proton-proton distances in single crystal protein conformations. *J. Mol. Biol.* **155**, 321–346.

Billeter, M., Kline, A. D., Braun, W., Huber, R. & Wüthrich, K. (1989). Comparison of the high-resolution structures of the α-amylase inhibitor tendamistat determined by nuclear magnetic resonance in solution and by X-ray diffraction in single crystals. *J. Mol. Biol.* **206**, 677–687.

Buchberger, A., Schroder, H., Buttner, M, Valencia, A. & Bukau, B. (1994). A conserved loop in the ATPase domain of the DnaK chaperone is essential for stable binding of GrpE. *Nature Struct. Biol.* **1**, 95–101.

Chellaiah, A., Davis, A. & Mohanakumar, T. (1993). Cloning of a unique human homologue of the *Escherichia coli* DnaJ heat shock protein. *Biochim. Biophys. Acta.* **1174**, 111–113.

Cheetham, M. E., Brion, J.-P. & Anderton, B. H. (1992). Human homologues of the bacterial protein DnaJ are preferentially expressed in neurons. *Biochem. J.* **284**, 469–476.

Cyr, D. M., Langer, T. & Douglas, M. G. (1994). DnaJ-like proteins: molecular chaperones and specific regulators of Hsp70. *Trends. Biochem. Sci.* **19**, 176–181.

Feldheim, D., Rothblatt, J. & Schekman, R. (1992). Topology and functional domains of Sec63p, an endoplasmic reticulum membrane protein required for secretory protein translocation. *Mol. Cell Biol.* **12**, 3288–3296.

Fesik, S. W. & Zuiderweg, E. R. P. (1988). Heteronuclear three-dimensional NMR spectroscopy. A strategy for simplification of homonuclear two-dimensional NMR spectra. *J. Magn. Reson.* **78**, 588–593.

Freeman, B. C., Myers, M. P., Schumacher, R. & Morimoto, R. I. (1995). Identification of a regulatory motif in Hsp70 that affects ATPase activity, substrate binding and interaction with HDJ-1. *EMBO J.* **14**, 2281–2292.

Frydman, J., Nimmesgern, E., Ohtsuka, K. & Hartl, F. U. (1994). Folding of nascent polypeptide chains in a high molecular mass assembly with molecular chaperones. *Nature*, **370**, 111–117.

Griesinger, C., Sørensen, O. W. & Ernst, R. R. (1985). Two-dimensional correlation of connected NMR transitions. *J. Am. Chem. Soc.* **107**, 6394–6396.

Griesinger, C., Otting, G., Wüthrich, K. & Ernst, R. R. (1988). Clean TOCSY for ^{1}H spin system identification in macromolecules. *J. Amer. Chem. Soc.* **110**, 7870–7872.

Güntert, P. & Wüthrich, K. (1991). Improved efficiency of protein structure calculations from NMR data using the program DIANA with redundant dihedral angle constraints. *J. Biomol. NMR*, **1**, 447–456.

Güntert, P. & Wüthrich, K. (1992). FLATT-A new procedure for high-quality baseline correction of

multidimensional NMR spectra. *J. Magn. Reson.* **96**, 403–407.

Güntert, P., Braun, W., Billeter, M. & Wüthrich, K. (1989). Automated stereospecific ^{1}H NMR assignments and their impact on the precision of protein structure determination in solution. *J. Amer. Chem. Soc.* **111**, 3997–4004.

Güntert, P., Braun, W. & Wüthrich, K. (1991a). Efficient computation of three-dimensional protein structures in solution from nuclear magnetic resonance data using the program DIANA and the supporting programs CALIBA, HABAS and GLOMSA. *J. Mol. Biol.* **317**, 517–530.

Güntert, P., Qian, Y. Q., Otting, G., Müller, M., Gehring, W. & Wüthrich, K. (1991b). Structure determination of the Antp(C39S) homeodomain from nuclear magnetic resonance data in solution using a novel strategy for the structure calculations with the programs DIANA, CALIBA, HABAS and GLOMSA. *J. Mol. Biol.* **217**, 531–540.

Güntert, P., Berndt, K. D. & Wüthrich, K. (1993). The program ASNO for computer-supported collection of NOE upper distance constraints as input for protein structure determination. *J. Biomol. NMR*, **3**, 601–606.

Hill, R. B., Flanagan, J. M. & Prestegard, J. H. (1995). ^{1}H and ^{15}N magnetic resonance assignments, secondary structure, and tertiary fold of *Escherichia coli* DnaJ(1-78). *Biochemistry*, **34**, 5587–5596.

Höhfeld, J., Minami, Y. & Hartl, F. U. (1995). Hip, a novel cochaperone involved in the eukaryotic Hsc70/Hsp40 reaction cycle. *Cell*, **83**, 589–598.

Kay, L. E., Keifer, P. & Saarinen, T. (1992). Pure absorption gradient enhanced heteronuclear single quantum correlation spectroscopy with improved sensitivity. *J. Am. Chem. Soc.* **114**, 10663–10665.

Kelley, W. L. & Landry, S. J. (1994). Chaperone power in a virus? *Trends. Biochem. Sci.* **19**, 277–278.

Langer, T., Lu, C., Echols, H., Flanagan, J., Hayer, M. K. & Hartl, F. U. (1992) Successive action of DnaK, DnaJ and GroEL along the pathway of chaperone-mediated protein folding. *Nature*, **356**, 683–689.

Liberek, K., Marszalek, J., Ang, D., Georgopoulos, C. & Zylicz, M. (1991). *Escherichia coli* DnaJ and GrpE heat shock proteins jointly stimulate ATPase activity of DnaK. *Proc. Natl Acad. Sci. USA*, **88**, 2874–2878.

Lyman, S. K. & Schekman, R. (1995). Interaction between BiP and Sec63 is required for the completion of protein translocation into the ER of *Saccharomyces cerevisiae*. *J. Cell Biol.* **131**, 1163–1171.

Marion, D., Ikura, M., Tschudin, R. & Bax, A. (1989). Rapid recording of 2D NMR spectra without phase cycling: application to the study of hydrogen exchange in proteins. *J. Magn. Reson.* **85**, 393–399.

Nagayama, K. & Wüthrich, K. (1981). Structural interpretation of vicinal proton-proton coupling constants $^{3}J_{\alpha\beta}$ in the basic pancreatic trypsin inhibitor measured by two-dimensional *J*-resolved NMR spectroscopy. *Eur. J. Biochem.* **115**, 653–657.

Oh, S., Iwahori, A. & Kato, S. (1993). Human cDNA encoding DnaJ protein homologue. *Biochim. Biophys. Acta*, **1174**, 114–116.

Ohtsuka, K. (1993). Cloning of a cDNA for heat-shock protein hsp40, a human homologue of bacterial DnaJ. *Biochem. Biophys. Res. Commun.* **197**, 235–240.

Rassow, J., Maarse, A. C., Krainer, E., Kubrich, M., Muller, H., Meijer, M., Craig, E. & Pfanner, N. (1994) Mitochondrial protein import: biochemical and genetic evidence for interaction of matrix hsp70 and the inner membrane protein MIM44. *J. Cell Biol.* **127**, 1547–1556.

Saiki, R. K., Gelfand, D. H., Stoffel, S., Scharf, S. J., Higuchi, R., Horn, G. T., Mullis, K. B. & Erlich, H. A. (1988). Primer-directed enzymatic amplification of DNA with a thermostable DNA polymerase. *Science*, **239**, 487–491.

Schlenstedt, G., Harris, S., Risse, B., Lill, R. & Silver, P. (1995). A yeast DnaJ homologue, Scj1p, can function in the endoplasmic reticulum with BiP/Kar2p via a conserved domain that specifies interactions with Hsp70s. *J. Cell Biol.* **129**, 979–988.

Szabo, A., Langer, T., Schroder, H., Flanagan, J., Bukau, B. & Hartl, F. U. (1994). The ATP hydrolysis-dependent reaction cycle of the *Escherichia coli* Hsp70 system-DnaK, DnaJ and GrpE. *Proc. Natl Acad. Sci. USA*, **91**, 10345–10349.

Szabo, A., Korszun, R., Hartl, F. U. & Flanagan, J. (1996). A zinc finger-like domain of the molecular chaperone DnaJ is involved in binding to denatured protein substrates. *EMBO J.* **15**, 408–417.

Szyperski, T., Güntert, P., Otting, G. & Wüthrich, K. (1992). Determination of scalar coupling constants by inverse Fourier transformation of in-phase multiplets. *J. Magn. Reson.* **99**, 552–560.

Szyperski, T., Pellecchia, M., Wall, D. Georgopoulos, C. & Wüthrich, K. (1994). NMR structure determination of the *Escherichia coli* DnaJ molecular chaperone: Secondary structure and backbone fold of the N-terminal region (residues 2-108) containing the highly conserved J domain. *Proc. Natl Acad. Sci. USA*, **91**, 11343–11347.

Ungewickell, E., Ungewickell, H., Holstein, S. E. H., Lindner, R., Prasad, K., Barouch, W., Martin, B., Greene, L. E. & Eisenberg, E. (1995). Role of auxilin in uncoating clathrin-coated vesicles. *Nature*, **378**, 632–635.

Wall, D., Zylicz, M. & Georgopoulos, C. (1994). The NH_2-terminal 108 amino acids of the *Escherichia coli* DnaJ protein stimulate the ATPase activity of DnaK and are sufficient for λ replication. *J. Biol. Chem.* **269**, 5446–5451.

Wagner, G. & Wüthrich, K. (1982). Sequential resonance assignments in protein ^{1}H nuclear magnetic resonance spectra. Basic pancreatic trypsin inhibitor. *J. Mol. Biol.* **155**, 347–366.

Weiner, S. J., Kollman, P. A., Nguyen, D. T. & Case, D. A., (1986). An all atom force field for simulations of proteins and nucleic acids. *J. Comp. Chem.* **7**, 230–252.

Wider, G., Lee, K. H. & Wüthrich, K. (1982). Sequential resonance assignments in protein ^{1}H nuclear magnetic resonance spectra. Glucagon bound to perdeuterated dodecylphosphocholine micelles. *J. Mol. Biol.* **155**, 367–388.

Wider, G., Hosur, R. V. & Wüthrich, K. (1983). Suppression of the solvent resonance in 2D NMR spectra of protein in H_2O solution. *J. Magn. Reson.* **52**, 130–135.

Wüthrich, K. (1986). *NMR of Proteins and Nucleic Acids*, Wiley, New York.

Xia, T.-H. (1992). Software for determination and visual display of NMR structures of proteins: the distance geometry program DGPLAY and the computer

graphics program CONFOR and XAM. *Diss. ETH Zurich* Nr. 9831.

Zinsmaier, K. E., Eberle, K. K., Buchner, E., Walter, N. & Benzer, S. (1994). Paralysis and early death in cysteine string protein mutants of *Drosophila*. *Science*, **263**, 977–980.

Edited by P. E. Wright

(Received 5 February 1996; received in revised form 12 April 1996; accepted 25 April 1996)

Supplementary material for this paper, comprising one table, is available from JMB Online.